Limnol. Oceanogr., 47(4), 2002, 1129–1136

Diffusion and advection within and around sinking, porous diatom aggregates

Helle Ploug[1]
Marine Biological Laboratory, University of Copenhagen, Strandpromenaden 5, DK-3000 Helsingør, Denmark

Susanna Hietanen and Jorma Kuparinen[2]
Finnish Institute of Marine Research (FIMR), P.O. Box 33, FIN-00931 Helsinki, Finland

Abstract

Fluid motion within and around sinking aggregates is an important factor in particle scavenging and solute exchange between sinking aggregates and the surrounding water and, hence, vertical fluxes and remineralization processes in the ocean. In the present study, we analyzed O_2 uptake rates in >2-mm porous diatom aggregates and in model aggregates impermeable to flow by measuring, on the same aggregates, the interface diffusive uptake rates with microsensors and the total (diffusive + advective) O_2 uptake rate by the Winkler method. The uptake rates were measured in a flow field similar to that experienced by sinking aggregates. The ratio of total O_2 uptake rate to diffusive uptake rate was 0.97 ± 0.10 (n = 14) in model aggregates impermeable to flow. In contrast, total O_2 uptake was similar to or higher than diffusive uptake rate calculated from the O_2 gradients at the aggregate–water interface in 85% of all field-sampled and roller tank diatom aggregates examined. The highest ratio of total O_2 uptake rate relative to diffusive uptake rate measured in <1-cm field-sampled diatom aggregates was 3.91 ± 1.39 (n = 22). Hence, diffusive O_2 uptake calculated from the O_2 gradients in aggregates is a conservative (minimum) estimate of total O_2 uptake. The estimated average fluid velocity through the cross-sectional area of field-sampled diatom aggregates, which could explain the measured differences in O_2 uptake, ranged between 5 and 40 μm s^{-1}. The average value was 16 μm s^{-1}, which was equal to 1.3% of aggregate sinking velocity.

A substantial fraction of primary production is removed from surface waters through coagulation processes and sedimentation of aggregates composed of living phytoplankton and detritus with an attached microbial community (Fowler and Knauer 1986; Alldredge and Silver 1988; Kiørboe et al. 1994). Particle scavenging and solute exchange between sinking aggregates and the surrounding water during sedimentation are, thus, important factors in vertical fluxes, remineralization, and nutrient retention in the mixed layer of the ocean and large lakes (Smith et al. 1992; Grossart and Simon 1998; Passow et al. 2001). The potential solute exchange between aggregates and the surrounding water is facilitated 5- to 20-fold in sinking aggregates impermeable to flow compared to that of suspended, nonsinking aggregates (Kiørboe et al. 2001; Ploug 2001). Colonization rates of 2.5-mm model aggregates by bacteria from the surrounding water increased three- to fourfold at flow rates similar to sinking velocities of marine snow compared to those in stagnant conditions (Fenchel 2001). Bacterial production increased 5- to 10-fold when aggregates were kept in suspension during incubations, compared to the rates measured under static conditions (Ploug and Grossart 1999, 2000). Hence, flow induced by aggregate sinking is important for the overall physical/chemical microenvironment in aggregates, as well as for colonization, growth, and respiration by attached biota. Theoretical studies have shown that interstitial flow through large, porous aggregates may be at least as significant as molecular diffusion in mass transfer within aggregates (Logan and Hunt 1987; Logan and Alldredge 1989). Experimental techniques that directly quantify interstitial fluid flow velocity within porous aggregates, however, have not been developed.

In the present study, we used microsensors and the Winkler technique to explore the relative potential importance of diffusion and interstitial flow through diatom aggregates. The radial diffusive interface O_2 fluxes to diatom aggregates and to model aggregates impermeable to flow were calculated from measured O_2 gradients in a flow field similar to that experienced by sinking aggregates. Total O_2 uptake rate was measured by the Winkler technique on the same aggregates. The O_2 uptake rates were analyzed and compared to those predicted by mass transfer theory.

Materials and methods

Aggregates—Model aggregates impermeable to flow were made by dripping a solution of agar dissolved in freshwater (1%, wt/wt) with bakers yeast (1%, wt/wt) at 40°C into parafine oil at room temperature as described in Cronenberg (1994). Sphere sizes ranging from 3.6 to 9.5 mm were made

[1] To whom correspondence should be addressed. Present address: Max Planck Institute for Marine Microbiology, Celsiusstr. 1, D-28359 Bremen, Germany (hploug@mpi-bremen.de).

[2] Present address: Department of Ecology and Systematics, Division of Hydrobiology, P.O. Box 65, FIN-0014 University of Helsinki, Finland.

Acknowledgments

We are grateful to H.-P. Grossart, who sampled diatom aggregates by SCUBA in the field. Software developed to determine the surface area of ellipsoids was written by Thomas Richter and is gratefully acknowledged. We thank Michael Olesen for the use of the automated Winkler titrator. This study was supported by grants from the Carlsberg Foundation (J.990513/20-542), the Danish Natural Science Research Council (SNF, J.9801391), the Alexander von Humboldt Foundation (IV DAN/1072992 STP) to H.P., and the Maj and Tor Nessling Foundation to S.H. We greatly appreciate comments by Bruce Logan and two anonymous reviewers on an earlier version of the manuscript.

by dripping one to three drops of agar/yeast solution on the same spot in the parafine oil with pipettes of different sizes. Aggregates were rinsed and suspended overnight at 15°C (i.e., each aggregate was placed on a thin glass thread submersed in water). These aggregates had an almost spherical shape and an evenly distributed respiration rate per aggregate volume. No carbon source was added to the surrounding water in order to keep respiration rates at the same level as those of similar-sized diatom aggregates.

Diatom aggregates were collected by SCUBA in Øresund (Denmark). They were mainly composed of *Skeletonema costatum*, *Chaetoceros* sp., and *Coscinodiscus* sp. O_2 uptake measurements were made within 2 h of sampling in most of these aggregates, whereas some were kept for 2 d in rotating vials to examine the uptake rates upon aging. In addition, diatom aggregates were formed from *Chaetoceros* or *Skeletonema* cultures grown at 15°C in a 16 : 8 h light : dark (LD) cycle on B-medium (Hansen 1989) diluted 10-fold. Silicate was added to a final concentration of 150 μM. The cultures were grown to the stationary phase and diluted 2.5-fold in natural seawater and incubated in 0.5-liter (14-cm-diameter) tanks on a roller table for >4 h (Shanks and Edmondson 1989). The *Skeletonema* culture was freeze–thawed before aggregate formation. The roller table was set at the lowest speed in which aggregates remained in suspension without contacting the walls of the tanks (0.025–0.04 s^{-1}). In this experimental system, aggregates form as a result of differential sedimentation rather than by shear after 100–1,000 s (Jackson 1994).

Diffusive oxygen uptake—A microelectrode with a 4-μm-wide tip, a stirring sensitivity of 0.3%, and a 90% response time of 0.8 s was used to measure oxygen gradients at the aggregate–water interface (Revsbech 1989). The electrode was attached to a micromanipulator, and its signal was measured by a picoamperemeter connected to the strip chart recorder (Kipp and Zonen) at high resolution (2 μM O_2 cm^{-1}). It was calibrated in air-saturated and anoxic water with sodium dithionite. Single aggregates were isolated by use of a wide-bore pipette and gently transferred to the chamber of a vertical flow system as described by Ploug and Jørgensen (1999). The flow chamber consisted of a 10-cm-long, circular Plexiglas tube (5 cm diameter) with a net extended in the middle of the tube. The net creates a relatively uniform flow field across the upper chamber. Aggregates were placed on the net, and the upward-directed flow velocity was adjusted by a needle valve until the aggregate was suspended and its sinking velocity was balanced by flow velocity. Aggregates were either freely suspended above the net or fixed on a thin glass thread above the net during measurements. It has been demonstrated that the presence of the glass needle does not interfere with measured gradients of flow and solutes in the vicinity of an aggregate when it is oriented away from the sites at which measurements are done (Kiørboe et al. 2001). Hence, the fluid motion and solute distribution in the vicinity of the aggregates under this experimental condition are equivalent to those in the vicinity of an aggregate sinking through the water column at a velocity equal to the water flow velocity (Kiørboe et al. 2001). The flow velocities were calculated from the volume of water passing through the chamber per unit time divided by the cross-sectional area of the chamber. Dimensions of individual aggregates and the relative distance between the microelectrode tip and the aggregate surface were measured through a dissection microscope with a calibrated ocular micrometer. All measurements were done at the steady state oxygen gradients. The temperature was 7°C, equal to the in situ temperature for field-sampled aggregates, whereas it was 15°C in other experiments. The water in the flow system was from the same source as that in which aggregates had formed. The water was filtered through microfiber glass filters (GF/C, Whatman) to avoid smaller particles collecting in the net of the flow system. A total of 48 aggregates from all sources were incubated for determination of respiration rates by the Winkler method immediately after microsensor measurements. Additional size-specific O_2 uptake rates were measured in yeast/agar spheres and in field-sampled diatom aggregates and compared with those measured by the Winkler method (*see below*).

Respiration rates were calculated from the oxygen gradients measured at multiple positions in the equatorial plane relative to the flow direction and at the downstream pole. The analytical solutions for oxygen distributions and diffusive fluxes at the aggregate–water interface were fitted to measured values by applying the solver routine of the spreadsheet program Excel 7.0 (Microsoft) as previously described (Ploug et al. 1997). In the case of a more ellipsoid shape, the aggregate surface area was calculated as described by Maas (1994). An oxygen diffusion coefficient ranging between 1.38×10^{-5} and 1.70×10^{-5} cm^2 s^{-1} was used in the calculations of oxygen fluxes depending on temperature and salinity (Broecker and Peng 1974).

The Winkler method—We followed the procedures of Winkler titration as previously described (Carritt and Carpenter 1966; Carignan et al. 1998). Five replicates were used to measure the concentration of oxygen at time zero (t_0). Yeast/agar aggregates and diatom aggregates were incubated individually in 6- or 11-ml gas-tight glass vials with glass stoppers. Each vial was filled with 0.2-μm-filtered water originating from the flow system, and one single aggregate was transferred to each vial by a wide-bore pipette afterwards. The vials were fixed in containers on a roller table and rotated around their shortest axis (ϕ: 1.0–2.0 cm) to let the aggregates sink during the incubations. Three replicates of blanks were incubated in parallel. Oxygen was precipitated by adding 400 μl mangane (II) chloride (3 M) and 400 μl sodium hydroxide (8 N) iodine (3 M) to the vials. Precipitate was allowed to settle for at least 2 h (more than halfway down the vial). Overlaying water (3 ml) was carefully removed, and 800 μl of 10 N sulfuric acid was added to dissolve the precipitate. The sample was then immediately titrated with 10 mM $Na_2S_2O_3$ on a computer-controlled photometric end-point detection system (716 DMS Titrino). The exact volume of each vial was measured previously by its increase in weight after it was filled with distilled water and closed. The temperatures were the same as during the microsensor measurements in all experiments. The accuracy of O_2 determinations was ± 2 μM, and the total decrease in O_2

concentration during the incubations was, on average, 60 μM (range: 10–150 μM).

Mass transfer theory—The relative importance of inertial and viscous forces acting in the vicinity of a sinking particle is expressed by the Reynolds number.

$$\mathrm{Re} = \frac{Ur_0}{\nu} \quad (1)$$

U is the sinking velocity (cm s^{-1}), r_0 is the particle or aggregate radius (cm), and ν is the kinematic viscosity of seawater (cm^2 s^{-1}).

The relative increase in mass transfer due to flow in the vicinity of sinking aggregates impermeable to flow, compared to that of suspended, nonsinking aggregates in stagnant water, is described by the (bulk) Sherwood number (Sh), and it increases with increasing Re (Kiørboe et al. 2001)

$$\mathrm{Sh} = 1 + 0.619\mathrm{Re}^{0.412}\mathrm{Sc}^{1/3} \quad (2)$$

where Re is defined with respect to aggregate radius; Sc is the dimensionless Schmidt number, equal to ν/D_w; and D_w (cm^2 s^{-1}) is the diffusion coefficient of the chemical solute in the surrounding water. Equation 2 is valid for all $\mathrm{Re} < 20$ because it is deduced by solving the diffusion/advection equations, as well as Navier–Stokes equations, numerically for creeping and laminar flow. Turbulent flow occurs at $\mathrm{Re} \gg 20$.

The radial local diffusive flux of oxygen at solid–water interfaces is expressed by (Sherwood et al. 1975).

$$J = -D_w\frac{dC}{dr} = D_w\frac{(C_\infty - C_0)}{\delta_{\mathrm{eff}}} \quad (3)$$

J is the flux (nmol O_2 cm^{-2} s^{-1}), and dC/dr is the radial concentration gradient at the aggregate–water interface, which can be extrapolated from the concentration at the surface, C_0 (nmol O_2 cm^3), to the bulk concentration, C_∞ (nmol O_2 cm^{-3}), in order to determine an effective diffusive boundary layer (DBL) thickness, δ_{eff} (cm).

The Sherwood number is 1 under stagnant conditions, and it increases when the average DBL thickness decreases due to flow in the vicinity of the aggregate (Ploug 2001). The local Sh and DBL thickness vary several-fold from the upstream to the downstream pole behind a sinking sphere impermeable to flow. The local Sh along the equator equals that of the bulk Sh; that is, the local Sh and DBL thickness along the equator represent the average values of the surface-integrated Sh and DBL thickness around sinking spheres impermeable to flow (Kiørboe et al. 2001; Ploug 2001). The radial local flux is dependent on the local DBL thickness during transport limitation of the biological processes. During reaction limitation and an evenly distributed activity of cells, however, the uptake rate is constant over the entire aggregate surface; therefore variations in local Sh reflect variations in surface concentration depending on local DBL thickness (Kiørboe et al. 2001; Ploug 2001).

When the oxygen concentration within aggregates is much higher than the half-saturation constant, K_m, for oxygen respiration (i.e., the respiration follows zero-order kinetics) and the aggregate is impermeable to flow, the flux becomes constant over the entire aggregate surface, and the total (area-integrated) diffusive uptake rate, Q_{dif}, is described by (Sherwood et al. 1975; Kiørboe et al. 2001)

$$Q_{\mathrm{dif}} = 4\pi r_0^2 D_w\frac{(C_\infty - C_0)}{\delta_{\mathrm{eff}}} = \mathrm{Sh}4\pi r_0 D_w(C_\infty - C_0) \quad (4)$$

where C_0 is the local O_2 concentration at the surface, Sh is the local Sherwood number, which can be expressed as the ratio of the aggregate radius (cm) to the local diffusive boundary layer thickness, δ_{eff} (cm), and $4\pi r_0^2$ is the surface area of the aggregate.

The O_2 uptake becomes transport limited when the oxygen demand is higher than the potential diffusive O_2 flux to an aggregate and the O_2 concentration at the surface and within aggregates is $\sim K_m$ (i.e., the respiration follows first-order kinetics). The half-saturation constant, K_m, for oxygen respiration is approximately 0.1–3 μM O_2 in heterotrophic bacteria, ciliates, and amoebae (Focht and Verstraete 1977; Fenchel and Finlay 1995). The average interface flux of O_2 increases proportional to the bulk Sh when the aggregate is impermeable to flow and the O_2 uptake is transport limited. The total uptake rate is then described by Eq. 4, where C_0 is the concentration at the surface and Sh is the bulk Sherwood number described by Eq. 2.

Interstitial fluid flow is a physical process that occurs independent of transport limitation in biological processes. We are not aware of any analytical solution that describes simultaneous advection and diffusion within aggregates. However, its potential effect on total mass transfer within aggregates was estimated from the measured difference between total and diffusive uptake rate. The potential mass transfer of O_2 by interstitial flow and diffusion within an aggregate was described by

$$Q_{\mathrm{tot}} = Q_{\mathrm{adv}} + Q_{\mathrm{dif}} \quad (5)$$

where Q_{adv} is the intra-aggregate O_2 consumption rate due to interstitial flow and Q_{dif} is the interface diffusive O_2 consumption rate. Q_{tot} was measured by the Winkler technique.

The averaged potential fluid velocity through the cross-sectional area of a porous, sinking aggregate (u_{agg}, cm s^{-1}) was estimated as

$$u_{\mathrm{agg}} = \frac{Q_{\mathrm{adv}}}{(C_\infty - C_{\mathrm{eff}})\pi r_0^2} \quad (6)$$

where $C_\infty - C_{\mathrm{eff}}$ was the measured difference in O_2 concentration between the bulk and that at the downstream pole (nmol O_2 cm^{-3}), πr_0^2 is the cross-sectional area of the aggregate (cm^{-2}), and Q_{adv} was measured in units of nmol O_2 s^{-1}.

Results

O_2 uptake in agar/yeast spheres—The total O_2 uptake measured by the Winkler titration method and the diffusive O_2 uptake in yeast/agar spheres measured by microsensors

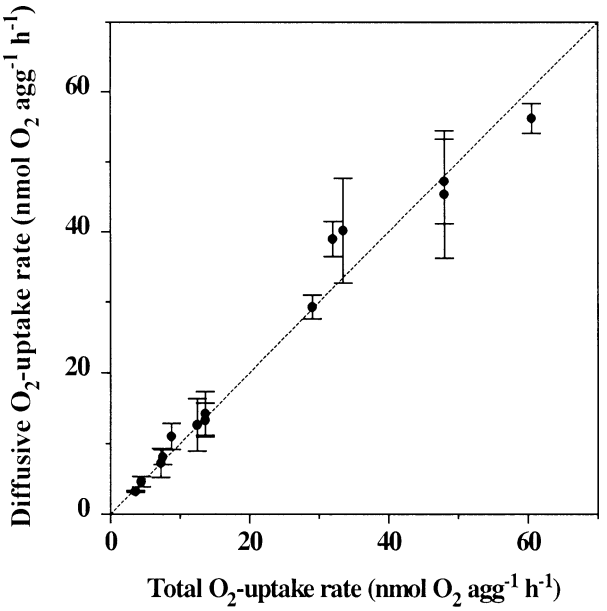

Fig. 1. Diffusive and total O_2 uptake rates measured in agar/yeast spheres. Each measuring point represents the mean value, with the standard deviation shown as bars (n = 3). The line represents the 1 : 1 ratio between the variables.

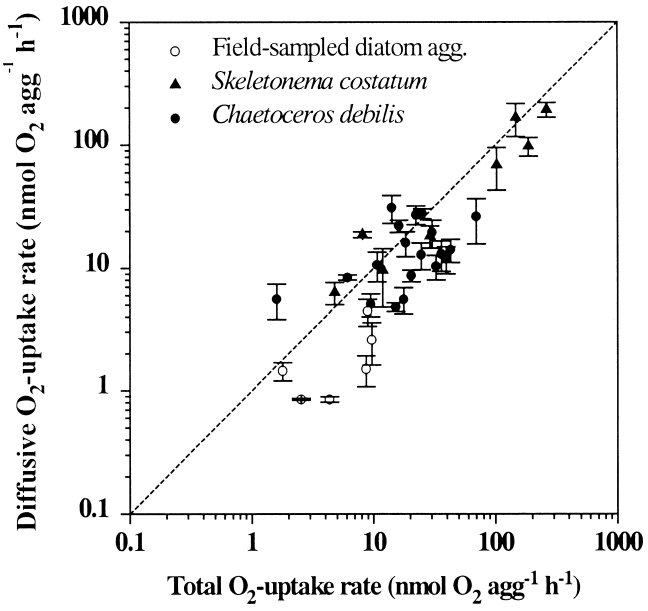

Fig. 2. Diffusive and total O_2 uptake rates measured in diatom aggregates. Each measuring point represents the mean value, with the standard deviation shown as bars (n = 4–6). The line represents the 1 : 1 ratio between the variables.

showed similar O_2 uptake rates (Fig. 1). This was expected because the agar/yeast spheres have a smooth surface, they are impermeable to flow, and O_2 uptake was not diffusion-limited during the incubations. These aggregates, therefore, served as a perfect control system of the two methods of respiration measurements.

O_2 uptake in diatom aggregates—Total O_2 uptake rate measured by the Winkler method and the interface diffusive O_2 uptake rate calculated from the measured O_2 gradients in the same diatom aggregates is shown (Fig. 2). The aggregates were incubated under conditions similar to those of the yeast/agar spheres. The total O_2 uptake rate was similar to or higher than the interface diffusive O_2 uptake rate calculated from the O_2 gradients in 85% of all aggregates examined. The microsensor method is sensitive to variability of fluxes around the aggregate. Measured diffusive O_2 fluxes were relatively similar along the equatorial plane relative to those at the downstream pole in lab-generated aggregates (Table 1). The equatorial diffusive flux was found to be significantly higher than that at the downstream pole in field-sampled aggregates ($P < 0.05$). The ratios of these fluxes, however, were 4- to 12-fold lower than those predicted at transport limitation of the biological processes (Ploug 2001). The ratio of aggregate radius to the local DBL thickness at the equator increases, as does the theoretical bulk Sh number, with increasing sinking velocity. Hence, the interface flux at the equatorial plane represents the average value of the surface-integrated flux to or from aggregates impermeable to flow (Kiørboe et al. 2001; Ploug 2001). The average diffusive O_2 uptake was, thus, calculated at the equator of aggregates (Fig. 2 and Table 2). The total O_2 uptake rate was significantly higher than the diffusive O_2 uptake rate in aggregates formed of *Chaetoceros debilis* and in field-sampled diatom aggregates ($P < 0.01$); thus, the respiration rates calculated on the assumption that diffusion is the sole mechanism of mass transfer within these diatom aggregates appears to be conservative (minimum) estimates.

A significantly higher total O_2 uptake rate, compared to the radial diffusive O_2 uptake rate, was only observed in field-sampled aggregates where O_2 concentrations at the aggregate surface were close to ambient concentrations. An example of the average oxygen distribution at the equator of a field-sampled diatom aggregate is shown in Fig. 3. The aggregate was 5.7 mm with a sinking velocity of 150 m d^{-1}. Its total O_2 uptake was 9.7 nmol O_2 h^{-1} as measured by the Winkler method. The ratio of aggregate radius to its local DBL thickness, δ_{eff}, was 8.3. Hence, the measured potential mass transfer due to flow and diffusion in the vicinity of an aggregate impermeable to flow increased 8.3-fold compared to that of a suspended, nonsinking, impermeable aggregate of similar size. The theoretical bulk Sh was 10.7 (i.e., 28% higher than the measured value). The O_2 concentrations measured at the aggregate–water interface, however, were higher

Table 1. Comparison of diffusive O_2 fluxes measured along the equatorial axis relative to the flow direction and at the downstream pole of the aggregates.

Aggregate source	Equatorial flux : downstream flux
Freeze–thawed diatoms (*Skeletonema costatum*)	1.01±0.27 (0.75–1.49); n=8
Living diatom culture (*Chaetoceros debilis*)	1.15±0.31 (0.67–1.69); n=20
Field-sampled diatom aggregates (chain-forming species)	1.86±0.83 (0.80–2.49); n=6

Table 2. Comparison of total O_2 uptake rate measured by the Winkler method and the interface diffusive O_2 uptake rate calculated from the oxygen gradients measured in the same aggregate. A significantly higher total uptake compared to the diffusive uptake, is indicated by (+), whereas a nonsignificant difference is indicated by (−).

Aggregate source	Total oxygen uptake: diffusive oxygen uptake	Total uptake rate >diffusive uptake rate
Yeast cells immobilized in 1% (wt/wt) agar spheres	0.97±0.10 (0.79–1.10); n=14	− P<0.05
Freeze–thawed diatoms (*Skeletonema costatum*)	1.21±0.49 (0.43–1.92); n=8	− P<0.05
Living diatom culture (*Chaetoceros debilis*)	1.84±1.14 (0.29–3.69); n=20	+ P<0.01
Field-sampled diatom aggregates	3.56±1.56 (1.24–6.17); n=6	+ P<0.01

than those expected from the total O_2 uptake measured if the aggregate was impermeable to flow. The radial diffusive uptake rate calculated from the measured O_2 gradient was 2.6 nmol O_2 h^{-1} (i.e., 3.7-fold lower than the total O_2 uptake rate measured).

The O_2 uptake rates measured by the Winkler method and the diffusive O_2 uptake rate in yeast/agar spheres and in field-sampled diatom aggregates are shown as a function of aggregate size in Fig. 4. The total O_2 uptake rate was similar to the diffusive O_2 uptake rate in yeast/agar spheres (Fig. 4A). The O_2 uptake rate (nmol O_2 agg^{-1} h^{-1}) could be described by $Q_{tot} = 122 \times vol - 0.45$ ($R^2 = 0.98$, $n = 42$), where vol is the sphere volume (cm^3). Hence, respiration was proportional to sphere volume. The radial diffusive interface O_2 flux to yeast/agar spheres was up to sixfold higher than that to similar-sized diatom aggregates, but it was similar to the total O_2 uptake of similar-sized diatom aggregates of >0.1 cm^3 (Fig. 4B). Hence, radial diffusion to diatom aggregates could have covered their oxygen demand even if these were impermeable to flow, as with the yeast/agar spheres. The total O_2 uptake rate in field-sampled diatom aggregates (nmol O_2 agg^{-1} h^{-1}) could be described by $Q_{tot} = 65.8(vol)^{0.67}$ ($R^2 = 0.89$, $n = 10$), where vol is the aggregate volume (cm^3). The diffusive O_2 uptake rate was described by $Q_{dif} = 20.0(vol)^{0.81}$ ($R^2 = 0.68$, $n = 16$). The total O_2 uptake rate was significantly higher than the diffusive O_2 uptake rate calculated from the oxygen gradients ($P < 0.01$). Total O_2 uptake rate was, on average, 3.91 ± 1.39 times higher than the radial diffusive O_2 uptake rate in all field-sampled diatom aggregates examined, as estimated from the regression lines (Fig. 4) and combined measurements of total and diffusive uptake rate in the same aggregates. The higher O_2 uptake measured by the Winkler method may be explained by interstitial flow through these aggregates.

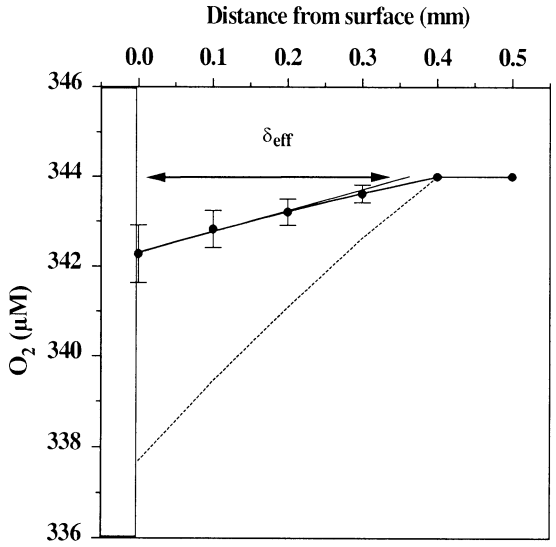

Fig. 3. Radial oxygen gradients along the equatorial plane of a field-sampled diatom aggregate. Each measuring point (symbols) represents the mean value, with the standard deviation shown as bars (n = 5). The lower curve represents the oxygen distribution as described by radial diffusion of O_2 to an impermeable aggregate with total O_2 uptake rates as measured by the Winkler method.

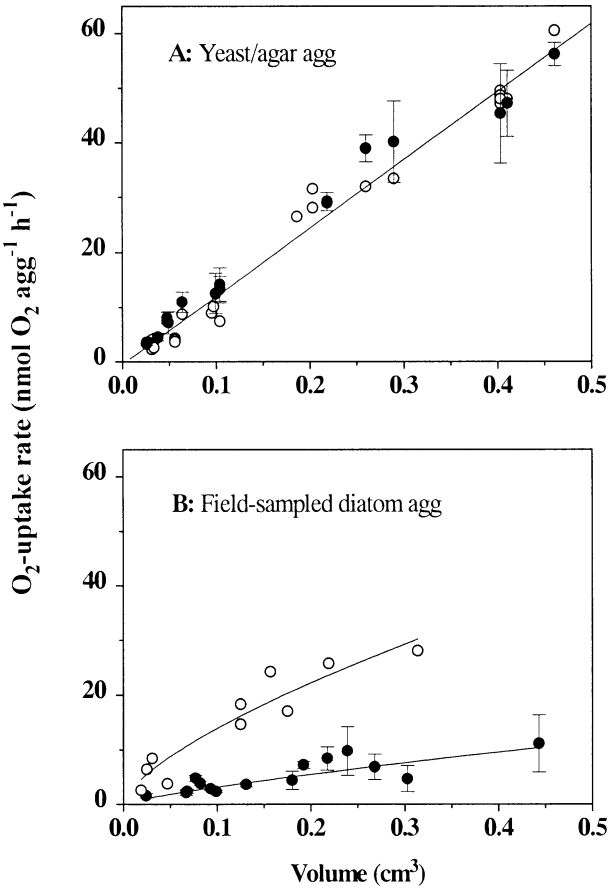

Fig. 4. Total O_2 uptake rates (open symbols) and diffusive O_2 uptake rates (closed symbols) as a function of aggregate volume. Each measuring point (closed symbols) represents the mean value, with the standard deviation shown as bars (n = 5).

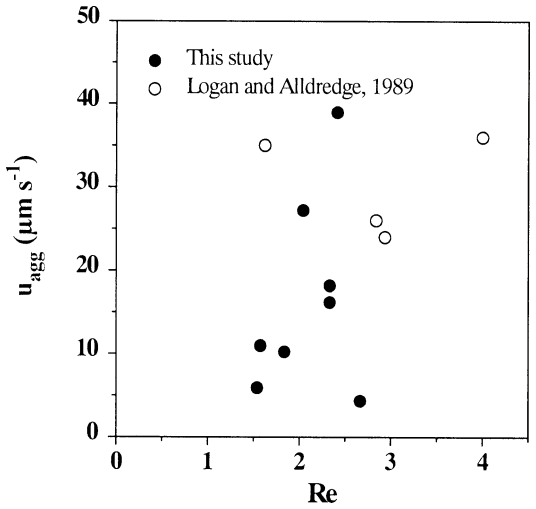

Fig. 5. Average interstitial fluid velocities estimated from total and diffusive O_2 uptake in field-sampled aggregates as a function of Re (closed symbols). Open symbols show the modeled interstitial fluid velocities in diatom aggregates with similar Re (Logan and Alldredge 1989).

The potential fluid velocity through field-sampled diatom aggregates was estimated from the total and diffusive O_2 uptake, assuming the O_2 uptake measured by the Winkler method represented diffusive uptake rate plus O_2 uptake due to interstitial fluid flow (Eqs. 5, 6). The estimated average fluid velocity through the cross-sectional area of the aggregates is shown as a function of Re in Fig. 5. The Reynolds numbers were calculated from measured aggregate size and sinking velocity and the temperature-dependent kinematic viscosity of seawater. The concentration difference between that of the bulk and that at the downstream pole was 6.4 ± 3.7 μM O_2, and the estimated interstitial fluid velocity ranged between 5 and 40 μm s^{-1}. Estimated intra-aggregate fluid velocity did not show any correlation to Re. The average value was 16.5 μm s^{-1}, equal to 1.3% of the average aggregate sinking velocity. The aggregate sinking velocity ranged between 55 and 170 m d^{-1}.

Discussion

Flow and diffusion in the vicinity of sinking aggregates impermeable to flow have been quantified from empirical measurements as well as from mass transfer theory (Kiørboe et al. 2001; Ploug 2001). It was shown that theoretical gradients of flow and oxygen at the aggregate–water interface agreed with those measured by microsensors and flow velocimetry in the flow system used in the present study (Kiørboe et al. 2001). In several studies, oxygen respiration rates have been calculated from measured O_2 gradients at the aggregate–water interface, assuming molecular diffusion is the sole process of mass transfer within the aggregates (Ploug et al. 1999; Ploug and Grossart 2000; Ploug 2001). In aggregates formed from a mixture of freeze–thawed diatoms, respiration rates varied between 1.4 and 14 nmol O_2 agg^{-1} h^{-1}. Hydrolysis and subsequent respiration by aggregate-attached biota could explain 78% of the observed time-dependent decrease in aggregate POC content when mass transfer within the aggregates was assumed to occur by molecular diffusion only (Ploug and Grossart 2000). The present study confirms that total O_2 uptake equals the radial diffusive O_2 uptake rate at the interface of sinking aggregates impermeable to flow. Low interstitial flow velocities may add to higher total mass transfer rates between sinking diatom aggregates and the surrounding water.

Recent studies have shown that fluid motion and diffusion in the vicinity of <1-cm sinking aggregates is sufficient to cover the oxygen demand by attached biota when the ambient O_2 concentration is above ~25 μM and mass transfer is assumed to occur by molecular diffusion within aggregates (Ploug 2001). O_2 uptake was, thus, determined by the number and activity of respiring cells within aggregates rather than by oxygen diffusion limitation at ambient O_2 concentrations above ~25 μM. Ambient O_2 concentrations decrease during incubation of aggregates in closed vials. The final concentration was >190 μM in the present study (i.e., well above the critical concentration at which respiration becomes diffusion limited in <1-cm aggregates impermeable to flow).

The ratio between total and diffusive O_2 uptake was independent of age of field-sampled aggregates. The data in Table 2 and Fig. 4 show the ratio of uptake rates in 2-d-old aggregates and freshly collected aggregates, respectively. Aggregates were incubated with 0.2-μm-filtered water, so respiration by free-living bacteria in the water phase can thus be excluded. The water in the flow system was prefiltered for particles, and release of additional nutrients by the 0.2-μm filtering process of the same water for Winkler incubations was presumably low. Bacterial growth rates, μ, have been shown to be 1.78 ± 0.02 d^{-1} in newly formed lab-generated diatom aggregates, and combined measurements of bacterial production and respiration on the same aggregates showed bacterial net growth efficiencies of 0.50 ± 0.10 (Grossart and Ploug 2001). Total O_2 uptake measured by the Winkler method is averaged over a longer time period (3 to 20 h), compared to the small-scale O_2 measurements (~0.5 h), and bacterial growth may largely explain the higher respiration rates in lab-generated aggregates obtained with the Winkler technique. The difference between total and diffusive uptake rates measured in field-sampled aggregates, however, was too high to be explained by bacterial growth (H.-P. Grossart pers. comm.).

Marine snow aggregates are fractal (Logan and Wilkingson 1990); hence, their dry weight and organic carbon and nitrogen content do not increase proportional to the apparent aggregate volume (Alldredge 1998). Consequently, the porosity increases with increasing aggregate size (Alldredge and Gotschalk 1988; Logan and Alldredge 1989). Respiration rates on aggregates measured in the present study also were not proportional to aggregate volume. A previous study has shown that respiration rate is proportional to aggregate POC and particulate organic nitrogen (PON) content rather than to apparent aggregate volume (Ploug and Grossart 2000). Aggregate porosity and sinking velocity of similar-sized aggregates vary largely in field-sampled aggregates, and transparent exopolymer particles (TEP) may limit fluid flow within aggregates (Alldredge and Gotschalk 1988;

Alldredge et al. 1993). Field-sampled diatom aggregates and aggregates composed of living *Chaetoceros* cells from the culture had lower respiration rates and appeared less compact compared to aggregates formed from freeze–thawed *S. costatum. Chaetoceros* cells form aggregates by producing TEP, which scavenge cells into aggregates, whereas the cells in *S. costatum* are sticky in themselves and coagulation, therefore, depends on cells sticking to each other (Kiørboe and Hansen 1993; Crocker and Passow 1995). The structure and exchangeable pore water content may, therefore, vary widely in diatom aggregates.

Fluid flow velocities through marine snow and microbial aggregates have not yet been directly quantified because of insufficient spatial resolution and sensitivity of existing experimental techniques. Previous theoretical models have assumed that fluid flow occurs across the aggregate surface in the equatorial plane (Adler 1981; Logan and Alldredge 1989; Stolzenbach 1993). Recent experimental studies of particle scavenging and aggregation, however, have indicated that flow occurs through macropores formed between clusters within fractal microbial aggregates rather than across the aggregate surface in the equatorial plane (Li and Logan 1997, 2001). The present study showed that DBL thickness largely persists in the equatorial plane of field-sampled diatom aggregates. The diffusive O_2 uptake rate, however, was on average 3.9-fold lower than the total measured O_2 uptake. The oxygen uptake of the aggregate-associated biota may, therefore, be explained by an advective oxygen supply through macropores in the interior of these aggregates, as predicted by the cluster-fractal model. Local fluid velocity through such macropores is presumably higher than the averaged fluid velocity through the cross-sectional area of the aggregates.

Particle scavenging, microbial colonization, hydrolysis, and remineralization processes in aggregates and their adjacent water are important small-scale processes that are believed to regulate vertical fluxes of sinking organic matter in the ocean (Smith et al. 1992; Azam and Long 2001; Kiørboe 2001). Small-scale fluid flow through marine snow aggregates implies more efficient scavenging of smaller particles by larger aggregates compared to aggregates that are impermeable to flow (Stolzenbach 1993; Li and Logan 1997, 2000). The present study showed that an average intra-aggregate fluid velocity ranging between 5 and 40 μm s^{-1} may occur in large porous aggregates during sedimentation. These flow velocities presumably lead to higher scavenging rates, as well as enhanced efflux of hydrolysis products from the aggregate to the surrounding water during sedimentation, compared to that of sinking aggregates impermeable to flow (Smith et al. 1992). Respiration on diatom aggregates also occurs at substantial rates. The total O_2 uptake ranged between 2.5 and 28 nmol O_2 agg^{-1} h^{-1} in 2.0- to 8.4-mm field-sampled diatom aggregates. The size-specific rates were 1.95 times the diffusive O_2 uptake measured in marine snow in the Southern California Bight (Ploug et al. 1999).

Bacterial production has been studied extensively in marine and lake snow (Alldredge et al. 1986; Simon et al. 1990; Grossart and Simon 1993). In comparison, respiration on aggregates has been studied to a much lesser extent, although respiration by aggregate-associated biota may partly regulate the sinking flux of organic carbon in the ocean (Ploug et al. 1999; Ploug and Grossart 2000; Azam and Long 2001). The incubation method combined with the Winkler titration technique presented in this study provide a simple and attractive tool for future respiration measurements in sinking marine and lake snow of >2 mm.

References

ADLER, P. M. 1981. Streamlines in and around porous particles. J. Colloid. Interface Sci. **81:** 513–535.

ALLDREDGE, A. L. 1998. The carbon, nitrogen and mass content of marine snow as a function of aggregate size. Deep-Sea Res. **45:** 529–541.

———, AND C. GOTSCHALK. 1988. In situ settling behavior of marine snow. Limnol. Oceanogr. **33:** 339–351.

———, AND M. W. SILVER. 1988. Characteristics, dynamics and significance of marine snow. Prog. Oceanogr. **20:** 42–82.

———, J. J. COLE, AND D. A. CARON. 1986. Production of heterotrophic bacteria inhabiting macroscopic organic aggregates (marine snow) from surface waters. Limnol. Oceanogr. **31:** 68–78.

———, U. PASSOW, AND B. E. LOGAN. 1993. The abundance and significance of a class of large, transparent organic particles in the ocean. Deep-Sea Res. **40:** 1131–1140.

AZAM, F, AND R. A. LONG. 2001. Sea snow microcosms. Nature **414:** 495–498.

BROECKER, W. S., AND T. H. PENG. 1974. Gas exchange rates between air and sea. Tellus **26:** 21–35.

CARIGNAN, R., A.-M. BLAIS, AND C. VIS. 1998. Measurements of primary production and community respiration in oligotrophic lakes using the Winkler method. Can. J. Fish. Aquat. Sci. **55:** 1078–1084.

CARRITT, D. E., AND J. H. CARPENTER. 1966. Comparison and evaluation of currently employed modifications of the Winkler method for determining dissolved oxygen in sea water J. Mar. Res. **24:** 286–318.

CROCKER, K. M., AND U. PASSOW. 1995. Differential aggregation of diatoms. Mar. Ecol. Prog. Ser. **117:** 249–257.

CRONENBERG, C. H. C. 1994. Biochemical engineering on a microscale: Biofilms investigated with needle-type glucose sensors. Ph.D thesis, Univ. of Amsterdam.

FENCHEL, T. 2001. Eppur si muove: Many water column bacteria are motile. Aquat. Microb. Ecol. **24:** 197–201.

———, AND B. J. FINLAY. 1995. Ecology and evolution in anoxic worlds. Oxford Univ. Press.

FOCHT, D. D., AND W. VERSTRAETE. 1977. Biochemical ecology of nitrification and denitrification. Adv. Microbiol. Ecol. **1:** 135–214.

FOWLER, S. W., AND G. A. KNAUER. 1986. Role of large particles in the transport of elements and organic compounds through the ocean water column. Prog. Oceanogr. **16:** 147–194.

GROSSART, H.-P., AND H. PLOUG. 2001. Microbial degradation of organic carbon and nitrogen on diatom aggregates. Limnol. Oceanogr. **46:** 267–277.

———, AND M. SIMON. 1993. Limnetic macroscopic organic aggregates (lake snow): Occurrence, characteristics, and microbial dynamics in Lake Constance. Limnol. Oceanogr. **38:** 532–546.

———, AND ———. 1998. Bacterial colonization and microbial decomposition of limnetic organic aggregates (lake snow). Mar. Ecol. Prog. Ser. **15:** 127–140.

HANSEN, P. J. 1989. The red tide dinoflagellate *Alexandrium tamarense*: Effects on behavior and growth of a tintinnid ciliate. Mar. Ecol. Prog. Ser. **53:** 105–116.

JACKSON, G. A. 1994. Particle trajectories in a rotating cylinder: Implications for aggregation incubations. Deep-Sea Res. **41:** 429–437.

KIØRBOE, T. 2001. Formation and fate of marine snow: Small-scale processes with large-scale implications. Sci. Mar. **65:** 57–71.

———, AND J. L. S. HANSEN. 1993. Phytoplankton aggregation formation—observations of patterns and mechanisms of cell sticking and the significance of exopolymeric material. J. Plankton Res. **15:** 993–1018.

———, C. LUNDSGAARD, M. OLESEN, AND J. L. S. HANSEN. 1994. Aggregation and sedimentation processes during a spring phytoplankton bloom—a field test to test coagulation theory. J. Mar. Res. **52:** 297–323.

———, H. PLOUG, AND U. H. THYGESEN. 2001. Fluid motion and solute distribution around sinking aggregates. I. Small scale fluxes and heterogenity of nutrients in the pelagic environment. Mar. Ecol. Prog. Ser. **211:** 1–13.

LI, X. Y., AND B. E. LOGAN. 1997. Collision frequencies of fractal aggregates with small particles by differential sedimentation. Eniviron. Sci. Tech. **31:** 1229–1236.

———, AND ———. 2001. Permeability of fractal aggregates. Water Res. **14:** 3373–3380.

LOGAN, B. E., AND A. L. ALLDREDGE. 1989. Potential for increased nutrient uptake by flocculating diatoms. Mar. Biol. **101:** 443–450.

———, AND J. R. HUNT. 1987. Advantages to microbes of growth in permeable aggregates in marine systems. Limnol. Oceanogr. **32:**1034–1048.

———, AND D. B. WILKINGSON. 1990. Fractal geometry of marine snow and other biological aggregates. Limnol. Oceanogr. **35:** 130–136.

MAAS, L. R. M. 1994. On the surface area of an ellipsoid and related integrals of elliptic integrals. Comput. Appl. Math. **51:** 237–249.

PASSOW, U., R. F. SHIPE, A. MURRAY, D. K. PAK, M. A. BRZEZINSKI, AND A. L. ALLDREDGE. 2001. The origin of transparent exopolymer particles (TEP) and their role in sedimentation of particulate matte. Cont. Shelf. Res. **21:** 327–346.

PLOUG, H. 2001. Small-scale oxygen fluxes and remineralization in sinking aggregates. Limnol. Oceanogr. **46:** 1624–1631.

———, AND H.-P. GROSSART. 1999. Bacterial production and respiration on suspended aggregates—a matter of the incubation method. Aquat. Microb. Ecol. **20:** 21–29.

———, AND ———. 2000. Bacterial growth and grazing on diatom aggregates: Respiratory carbon turnover as a function of aggregate size and sinking velocity. Limnol. Oceanogr. **45:** 1467–1475.

———, AND B. B. JØRGENSEN. 1999. A net-jet flow system for mass transfer and microsensor studies in sinking aggregates. Mar. Ecol. Prog. Ser. **176:** 279–290.

———, M. KÜHL, B. BUCHHOLZ, AND B. B. JØRGENSEN. 1997. Anoxic aggregates—an ephemeral phenomenon in the pelagic environment. Aquat. Microb. Ecol. **13:** 285–294.

———, H. P. GROSSART, F. AZAM, AND B. B. JØRGENSEN. 1999. Photosynthesis, respiration and carbon turn-over in sinking marine snow from surface waters of Southern California: Implications for the carbon cycle in the ocean. Mar. Ecol. Prog. Ser. **179:** 1–11.

REVSBECH, N. P. 1989 An oxygen microelectrode with a guard cathode. Limnol. Oceanogr. **34:** 474–478.

SHANKS, A. L., AND E. W. EDMONDSON. 1989. Laboratory made artificial marine snow: A biological model of the real thing. Mar. Biol. **101:** 463–470.

SHERWOOD, T. K., R. L. PIGFORD, AND C. R. WILKE. 1975. Mass transfer. McGraw-Hill Book Company.

SIMON, M., A. L. ALLDREDGE, AND F. AZAM. 1990. Bacterial dynamics on marine snow. Mar. Ecol. Prog. Ser. **65:** 205–211.

SMITH, D. C., M. W. SILVER, A. L. ALLDREDGE, AND F. AZAM. 1992. Intensive hydrolytic activity on marine aggregates and implications for rapid particle dissolution. Nature **359:** 139–141.

STOLZENBACH, K. D. 1993. Scavenging of small particles by fast-sinking porous aggregates. Deep-Sea Res. **40:** 359–369.

Received: 12 July 2001
Accepted: 31 January 2002
Amended: 19 February 2002